Int. J. Radiation Oncology Biol. Phys., Vol. 60, No. 3, pp. 748–758, 2004

0360-3016/04/$–see front matter

ELSEVIER

doi:10.1016/j.ijrobp.2004.04.037

CLINICAL INVESTIGATION **Lung**

REGIONAL DIFFERENCES IN LUNG RADIOSENSITIVITY AFTER RADIOTHERAPY FOR NON–SMALL-CELL LUNG CANCER

YVETTE SEPPENWOOLDE, PH.D., KATRIEN DE JAEGER, M.D., M.SC., LIESBETH J. BOERSMA, M.D., PH.D., JOSÉ S. A. BELDERBOS, M.D., AND JOOS V. LEBESQUE, M.D., PH.D.

Department of Radiotherapy, The Netherlands Cancer Institute, Antoni van Leeuwenhoek Hospital, Amsterdam, The Netherlands

Purpose: To study regional differences in lung radiosensitivity by evaluating the incidence of radiation pneumonitis (RP) in relation to regional dose distributions.

Methods and Materials: Registered chest CT and single photon emission CT lung perfusion scans were obtained in 106 patients before curative or radical radiotherapy for non–small-cell lung cancer. The mean lung dose (MLD) was calculated. The single photon-emission CT perfusion data were used to weigh the MLD with perfusion, resulting in the mean perfusion-weighted lung dose. In addition, the lungs were geometrically divided into different subvolumes. The mean regional dose (MRD) for each region was calculated and weighted with the perfusion of each region to obtain the mean perfusion-weighted regional dose. RP was defined as respiratory symptoms requiring steroids. The incidence of RP for patients with tumors in a specific subvolume was calculated. The normal tissue complication probability (NTCP) parameter values for the TD_{50}, and an offset NTCP parameter for tumor location were fitted for both lungs and for each lung subvolume to the observed data using maximum likelihood analysis.

Results: The incidence of RP correlated significantly with the MLD and MRD of the posterior, caudal, ipsilateral, central, and peripheral lung subvolumes (p between 0.05 and 0.002); no correlation was seen for the anterior, cranial, and contralateral regions Similarly, a statistically significant correlation was observed between the incidence of RP and the perfusion-weighted MLD and perfusion-weighted MRD for all regions, except the anterior lung region. For this region, the dose–effect relation improved remarkably after weighting the local dose with the local perfusion. A statistically significant difference ($p = 0.01$) in the incidence of RP was found between patients with cranial and caudal tumors (11% and 40%, respectively). Therefore, a dose-independent offset NTCP parameter for caudal tumors was included in the NTCP model, improving most correlations significantly, confirming that patients with caudal tumors have a greater probability of developing RP.

Conclusion: The incidence of RP correlated significantly with the MLD and MRD of most lung regions, except for the anterior, cranial, and contralateral regions. Weighting the local dose with the local perfusion improved the dose–effect relation for the anterior lung region. Irradiation of caudally located lung tumors resulted in a greater risk of RP than irradiation of tumors located in other parts of the lungs. **© 2004 Elsevier Inc.**

Radiation pneumonitis, NTCP, Lung cancer, Radiotherapy.

INTRODUCTION

Estimation of the probability of developing radiation pneumonitis (RP) after treatment with high-dose radiotherapy (RT) is important for patients with inoperable non–small-cell lung cancer (NSCLC). RP is a severe complication that occurs within the first 6 months after RT and may be life-threatening. Clinical symptoms range from fever, dyspnea, and cough to death from respiratory failure. The risk of developing RP limits the maximal radiation dose that can be safely delivered to thoracic tumors. Knowledge of the relationship between the three-dimensional dose distribution and the incidence of RP is essential for designing a treatment plan that maximizes the tumor dose and minimizes the normal tissue complication probability (NTCP). Most theoretical models that have been developed to estimate the risk of RP were based on three-dimensional dose distributions (1–8). Dose–volume histograms were con-

Reprint requests to: Katrien De Jaeger, M.D., M.Sc., Department of Radiotherapy, The Netherlands Cancer Institute, Antoni van Leeuwenhoek Hospital, Plesmanlaan 121, Amsterdam 1066 CX The Netherlands. Tel: (+31) 20-512-2118; Fax: (+31) 20-669 1101; E-mail: k.d.jaeger@nki.nl

Supported by the Dutch Cancer Society (Grant 99-2043). Y. Seppenwoolde and K. De Jaeger contributed equally to this study.

Acknowledgments—We thank Guus Hart for statistical advice, Dr. S. H. Muller for useful discussions on SPECT, and Corinne Goedbloed, Kenneth Pengel, and Maddalena Rossi for data management support.

Received Dec 10, 2003, and in revised form Apr 12, 2004. Accepted for publication Apr 13, 2004.

structed considering either each lung as a single organ or both lungs as one organ. These models, however, do not take into account possible spatial differences in lung radiosensitivity. Graham *et al.* (9) found in a study of 70 lung cancer patients that the incidence of RP correlated with the location of the tumor, irrespective of the dose–volume parameters. Patients with lower lobe tumors had a much greater risk of RP than those with upper lobe tumors. In a more recent study by Yorke *et al.* (10), commonly used dosimetric and NTCP models were used to evaluate possible regional differences in radiosensitivity. Equally strong correlations were found between RP and mean doses in the lower portion of the lungs and the ipsilateral lung, but not with the mean dose in the upper portion or contralateral lung.

Also the results in animal models have indicated that the caudal lung regions are more sensitive to radiation. Graham *et al.* (8), Moiseenko *et al.* (11), and Travis *et al.* (12) found that the lung base of mice is more sensitive than the apex using either breathing rate or lethality as assays of RP. In addition, Khan *et al.* (13) reported that irradiation of the lower lung resulted in more DNA damage than irradiation of the upper lung in rats.

The purpose of this study was to analyze the regional differences in lung radiosensitivity by determining the regional dose–effect relations for RP. Therefore, we fitted the NTCP parameter values of TD_{50}, m, and an offset NTCP parameter for tumor location (14) for several different lung regions to the observed incidence of RP in a large group of patients treated for lung cancer. To study whether regional differences in function (as assessed by registered single photon emission CT [SPECT] lung perfusion scans) influenced the NTCP parameter values, we reanalyzed the data after weighting the locally delivered radiation dose with the local perfusion.

METHODS AND MATERIALS

A total of 106 patients with medically inoperable or locally advanced NSCLC and good prognostic factors (weight loss $<10\%$, Eastern Cooperative Oncology Group performance status ≤ 2) were included in this study (Table 1). The eligibility criteria were the presence of visible tumor on a diagnostic chest CT scan, availability of CT and SPECT scans before RT (all acquired in the treatment position, which was supine with the arms raised above the head in a forearm support), and a minimal follow-up of 6 months. Of these 106 patients, 58 were treated with conventional doses (49.5–70 Gy, 2 Gy/fraction) and 48 were treated according to the protocol of a dose-escalation study (15), with doses between 60.8 and 94.5 Gy (2.25 Gy/fraction). Thirty-six patients received elective nodal RT and 70 received involved-field RT. Most patients were treated with two to five coplanar nonintensity-modulated beams. All treatments were delivered using 8-MV photons. Only 6 of 106 patients received chemotherapy with an interval of at least 4 weeks until the start of RT. The scheme consisted of a platinum compound combined with gemcitabine. The local hospital ethics committee approved the study and all patients provided written informed consent.

Table 1. Patient, tumor, and treatment characteristics

Gender (*n*)	
Male	79
Female	27
Age (y)	
Median	73
Range	37–88
Performance status (ECOG) (*n*)	
0–1	94
2	12
Smoking history (*n*)	
Nonsmoker	8
Former smoker	69
Current smoker	29
Chronic obstructive pulmonary disease (*n*)	
Yes	58
No	48
Previous lung surgery (*n*)	3
Cardiac morbidity (*n*)	16
Tumor stage (*n*)	
I (IA/IB)	29 (13/16)
II (IIA/IIB)	17 (2/15)
III (IIIA/IIIB)	60 (33/27)
GTV before RT (cm^3)	
Mean	111.7
Range	2–901
RT dose to GTV (Gy)	
Mean	72.7
Range	49.5–92.5
Chemotherapy before RT (*n*)	6
RT alone (*n*)	100

Abbreviations: ECOG = Eastern Cooperative Oncology Group; GTV = gross tumor volume; RT = radiotherapy.

Data acquisition

Before RT, SPECT lung perfusion and chest CT scans were obtained. In this study, lung perfusion was considered to be representative of the regional functionality of the lung. To obtain lung SPECT perfusion scans, ^{99m}Tc-labeled albumin microaggregates were injected intravenously. The relatively large albumin is trapped in the small capillaries in the lungs. For SPECT acquisition, a dual-head gamma camera (ADAC Genesys or ADAC Vertex) equipped with medium-energy general-purpose collimators was used. After administration of about 4 mCi of ^{99m}Tc-macroaggregated albumin to the patient in the supine position, SPECT lung perfusion scans were made (scan time approximately 15 min). The scans were reconstructed using filtered back projection with software provided by the manufacturer. The number of voxels was $64 \times 64 \times 64$, and the voxel size was approximately $6 \times 6 \times 6$ mm^3. The resolution of the reconstructed SPECT images was 20–25 mm (full width at half maximum), as measured with a line source filled with ^{99m}Tc. All local SPECT values were normalized to the average number of SPECT counts, as described previously (16).

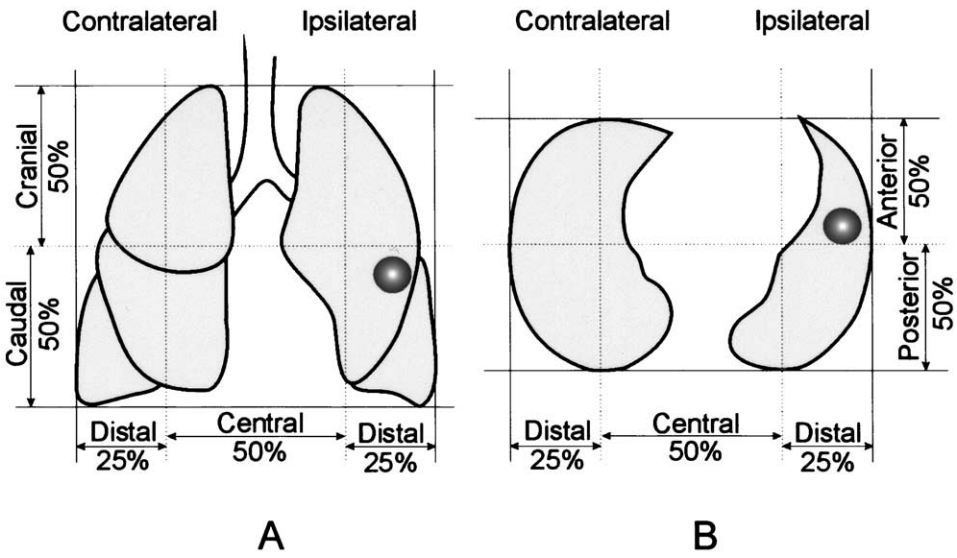

Fig. 1. Schematic overview of construction of different lung regions in (A) frontal and (B) axial views. See text for details and also Table 4.

A CT scan with a 5-mm slice thickness was made within 1 week of the accompanying SPECT scan, with the patient in the same position (CT scanners used included Siemens, Somatom Plus, or General Electric LX1). Both CT and SPECT acquisition were performed under normal breathing conditions (no "breathhold" procedure) and included the entire lung volume.

Lung contour matching

To obtain lung contours, the CT images were segmented by binary thresholding. The threshold value was chosen at a density of 0.7 g/mL. The gross tumor volume (GTV) was excluded from the lung volume. For correlation of the CT and SPECT scans, chamfer matching (17) was applied to the lung contours. The lung contours from SPECT were constructed by segmenting the lung perfusion scans by binary thresholding using an adjustable threshold. During matching with the lung contours in the CT scan, the best fitting threshold was obtained. After correlating the SPECT lung perfusion scans with the CT images, a first order Chang-like (18) attenuation correction (19) was applied to the SPECT perfusion scans using the CT density inhomogeneities.

Dose calculation

Computed tomography–based dose calculations were performed, as described previously (20), using a three-dimensional treatment planning system (U-MPlan, University of Michigan), with tissue inhomogeneity correction based on an equivalent pathlength algorithm. For inhomogeneous dose distributions, the dose per fraction differs greatly for different regions of the lungs. To take this dose/fraction effect into account, the physical dose distribution was converted into the normalized total dose distribution (21), using the linear-quadratic model with an α/β ratio of 3 Gy (22). The normalized total dose is defined as the total biologic equivalent dose given in fractions of 2 Gy (23). All radiation doses in the data presented in this paper were biologic equivalent doses.

Complications

The severity of RP occurring in the first 6 months after treatment was scored according to the Southwest Oncology Group toxicity criteria. Grade 1 (mild) RP applies when infiltrative radiographic changes within the radiation field (on chest X-ray or CT scan) are observed or symptoms develop that do not require steroids. Grade 2 (moderate) is scored when treatment with steroids is required. For Grade 3 (severe), oxygen is needed, and for Grade 4 (life-threatening), assisted ventilation is required because of persistent cough and/or dyspnea complaints. For all patients the follow-up time was at least 6 months. Because the scoring of Grade 1 RP is clinically irrelevant and unreliable, the endpoint of this study was RP of Grade 2 or worse. Grade 2 RP according to the Southwestern Oncology Group corresponds to Grade 3 according to the Radiation Therapy Oncology Group scoring system (10).

Dose–volume parameters of total lung and subvolumes

We have previously reported that the incidence of RP strongly depends on the dose distribution, with no relation to the prescribed dose (14). Also, the fraction sizes used (2 and 2.25 Gy) have too little variation to evaluate the impact of fraction size on the risk of RP.

First, we determined the dosimetric parameters considering both lungs as one organ. The mean lung dose (MLD) was defined as the average dose throughout the total lung volume minus the GTV. Subsequently, the MLD was weighted with the local perfusion resulting in the mean perfusion-weighted lung dose (MpLD).

In each patient, the total lung volume was also divided

into several regions (Fig. 1). The ipsilateral lung was defined as the lung containing the largest fraction of the GTV. The opposite lung was defined as contralateral. The linear distance between the most cranial and caudal voxels containing lung tissue in the CT scan was measured, and a plane halfway between them was defined to obtain the cranial and caudal lung subvolumes. Similarly, the distance between the most anterior and posterior voxels containing lung tissue was measured, and a plane halfway divided the lung into the anterior and posterior lung subvolumes. Furthermore, two planes were defined at 25% and 75% between the most left and right lung voxels to determine the central and peripheral lung regions. These geometrically defined lung subvolumes are complementary but do not correspond to the anatomic lobes of the lung, and the volumes of the opposite regions are not necessarily equal.

In each patient, we calculated for each lung subvolume the mean regional dose (MRD). The mean regional perfusion was calculated by averaging the local perfusion over all voxels within that region. The mean perfusion-weighted regional dose (MpRD) was calculated by first multiplying the local dose with the local perfusion.

The position of the GTV was determined in relation to the above-mentioned regions. A tumor was considered to be in a certain region if the bulk of the GTV was located in that region. If the GTV volume was located on more than three CT slices in the opposite region, the location was defined as "halfway."

Normal tissue complication probability

The NTCP was calculated from the MLD, MpLD, MRD, or MpRD, assuming a sigmoid (integrated normal distribution) relation between the complication and MLD, MpLD, MRD, or MpRD:

$$\mathrm{NTCP} = \frac{1}{\sqrt{2\pi}} \int_{-\infty}^{t} e^{\frac{-x^2}{2}}\, dx + \text{offset parameter}$$

with

$$t = \frac{M(p)RD - TD_{50}}{m \cdot TD_{50}}$$

The shape of the NTCP relation is determined by three parameters (14): TD_{50}, m, and an offset. TD_{50} represents the dose that will cause a 50% complication rate (without the offset). The parameter m is the slope parameter (steepness of the curve increases with decreasing m). In this article, a dose-independent offset NTCP parameter was used to account for tumor location.

Statistical analysis

First, we studied whether a statistically significant difference in the incidence of RP was present between patients with tumors in opposite lung regions, using a chi-square test. In addition, we tested whether differences existed in the MLD and MpLD between patients with tumors in opposite lung regions using the two-tailed *t* test.

Regional differences in perfusion were tested using the paired two-tailed *t* test. The correlation between the MRD and MLD was tested by calculating the Pearson correlation coefficient. Subsequently, for each region, we studied whether the MRD correlated with the incidence of RP. Therefore, we fitted the NTCP model to the observed data for the whole lung and for the different subvolumes. In a maximum likelihood analysis (5), the best fitting parameter values were those for which the likelihood function L has a maximum. The value of L is a measure for the agreement between the measured results and the results as predicted by the model, which, in our case, were the NTCP values calculated from the associated MRDs. Given the model parameter values for a data set containing N patients, the N-associated NTCP values P_i ($i = 1..N$) can be calculated. Each patient in the data set has an associated measured endpoint ep, which is either 0 or 1. The expression for the natural logarithm of the likelihood function L is

$$\ln(L) = \ln\left(\prod_{i=1}^{N} L_i\right) = \sum_{i=1}^{N} \ln(L_i)$$

$$= \sum_{i=1}^{N} [ep_i \ln(P_i) + (1 - ep_i)\ln(1 - P_i)]$$

Fitting of the model was performed by automatically adjusting TD_{50}, m, and the offset to maximize ln(L) using the Excel Solver Add-In. The significance of these relationships was determined with binary logistic regression using Statistical Package for the Social Sciences, version 9 (site license). To calculate the impact of the offset, a likelihood ratio test was performed (24) by comparing the maximal log likelihood values of the model with the offset to that of the model without the offset. Adding an extra parameter (degree of freedom) to a model will always result in an increase of the maximal log likelihood. To correct for this effect, an increase in the maximal log likelihood was only considered statistically significant when this value was equal to or larger than one-half of the χ^2 value associated with a confidence level of 0.05 and one extra degree of freedom (24).

RESULTS

Of the 106 patients with NSCLC enrolled in this study, 17 developed RP of at least Grade 2, corresponding to a crude incidence of 16%. One patient experienced a Grade 3 and another patient a Grade 4 complication within 6 months of follow-up.

Tumor location

The tumor location was not distributed equally over the different lung regions (Table 2). In 15 patients only, the tumor was located in the caudal lung region. In 6 of these

Table 2. Comparison of incidence of RP, MLD, and MpLD between patients with tumors in opposite lung regions

Tumor localization	Tumors (n)	Patients with RP Grade ≥2 (n)	RP incidence (%)	p	Average MLD (Gy)	Average MpLD (Gy)
Anterior	23	2	9		17 (5)	15 (5)
Halfway	30	5	17	0.5	17 (5)	15 (5)
Posterior	53	10	19		15 (5)	14 (5)
Cranial	72	8	11		15 (5)	13 (5)
Halfway	19	3	16	0.01*	17 (4)	16 (4)
Caudal	15	6	40		15 (5)	16 (5)
Left	44	7	16	1	16 (5)	15 (4)
Right	62	10	16		16 (5)	14 (5)
Central	57	10	18		17 (5)	15 (5)
Halfway	27	3	11	0.7	16 (5)	16 (5)
Peripheral	22	4	18		12 (5)	12 (5)

Abbreviations: RP = radiation pneumonitis; MLD = mean lung dose; MpLD = mean perfusion-weighted lung dose.
Data presented as average value, with SD in parentheses, unless otherwise noted.
Difference in incidence of RP between opposite lung regions tested using chi-square test.
* Statistically significant at $p \leq 0.05$.

patients, RP occurred, corresponding to an incidence of 40%. This incidence was significantly greater ($p = 0.01$) than for those with tumors located in the middle and cranial part of the lungs (incidence 16% and 11%, respectively). This difference could not be explained by a difference in the MLD, because the MLD was similar for these groups (Table 2). The MpLD, however, was somewhat greater for patients with caudal tumors than for patients with cranial tumors (16 Gy vs. 13 Gy, $p < 0.05$). Although patients with central and peripheral tumors had a similar incidence of RP, the MLD and the MpLD were significantly greater ($p < 0.001$ and $p < 0.05$, respectively) in patients with central tumors than in those with peripheral tumors. For patients with tumors located in the other opposite regions (left vs. right, anterior vs. posterior), neither the incidence of RP nor the MLD and MpLD were significantly different statistically (Table 2).

Regional perfusion

The mean local perfusion in different lung regions was calculated for all patients (Table 3). The mean perfusion, averaged over all patients, was greater in the contralateral, peripheral, and posterior lung regions than in the ipsilateral, central, and anterior lung regions ($p < 0.001$). Between the cranial and caudal lung regions, there could be large differences in individual patients, but, on average, the difference in the mean regional perfusion was not statistically significant ($p = 0.15$). The average difference was largest between the anterior and posterior and ipsilateral and contralateral lung regions (Table 3). Because the volumes of the opposite lung regions were not equal (Table 4), the average perfusion of two opposite regions was not necessarily equal to 1 (Table 3).

Table 3. Mean perfusion in different lung regions averaged over all patients

Region	Mean regional perfusion	p
Anterior	0.85 (0.12)	<0.001
Posterior	1.10 (0.08)	
Cranial	0.98 (0.19)	0.15
Caudal	1.03 (0.18)	
Ipsilateral	0.88 (0.20)	<0.001
Contralateral	1.11 (0.26)	
Central	0.96 (0.10)	<0.001
Peripheral	1.04 (0.08)	

Data presented as average value, with SD in parentheses.

Mean regional dose

The mean lung dose MLD for the entire lung volume was 16 Gy, averaged over all patients. The ipsilateral lung had the highest MRD (26 Gy) and the contralateral the lowest (6 Gy; Table 4), because beam incidences were often chosen such that RT of the contralateral lung was avoided. The differences between the other lung regions were smaller, with the cranial region having a greater MRD than the caudal and the central subvolumes having a greater MRD than the peripheral (Table 4). This was because most tumors were situated in the regions that received a greater mean dose. The anterior and posterior lung regions had, on average, almost the same mean dose, although more tumors were located in the posterior region (Table 2). In all regions, the MRD correlated significantly with the MLD; the correlation was best for the posterior region ($r^2 = 0.93$; Fig. 2A) and worst for the cranial and caudal regions ($r^2 = 0.64$ and 0.59, respectively; Fig. 2B)

Mean perfusion-weighted regional dose

The MpLD was, on average, 14 Gy and slightly lower than the average MLD. The MpRDs were, on average, lower than the MRDs (Table 4), because perfusion defects were usually localized near the tumor and received a high dose. Well-perfused regions (e.g., in the contralateral lung) often received a lower dose or no dose at all. For some of

Table 4. Parameter values of NTCP model for each lung region

Region/volume (L)	Dose parameter	MpRD (Gy)	TD_{50} (Gy)	m	Offset (%) for caudal tumors	p	
						Binary logistic*	χ^2 offset†
Entire lung/4.3 (1.3)	MLD	16 (5)	30	0.45		0.02‡	
			30	0.37	28	0.002‡	0.01‡
	MpLD	14 (5)	27	0.45		0.01‡	
Anterior/1.8 (0.7)	MRD	17 (7)	49	0.66		0.2	
	MpRD	13 (6)	33	0.58		0.04‡	
			37	0.54	27	0.006‡	0.01‡
Posterior/2.5 (0.8)	MRD	15 (5)	26	0.37		0.002‡	
			25	0.31	27	0.0002‡	0.01‡
	MpRD	15 (6)	30	0.48		0.02‡	
			34	0.48	23	0.007‡	0.04‡
Cranial/2.0 (0.8)	MRD	23 (9)	∞	1.00		0.9	
	MpRD	19 (8)	∞	0.92		0.8	
Caudal/2.3 (0.8)	MRD	10 (7)	31	0.66		0.02‡	
	MpRD	10 (8)	42	0.75		0.07	
Ipsilateral/2.1 (0.7)	MRD	26 (9)	55	0.51		0.03‡	
			57	0.44	27	0.004‡	0.02‡
	MpRD	22 (9)	58	0.60		0.05‡	
Contralateral/2.2 (0.8)	MRD	6 (4)	43	0.86		0.6	
	MpRD	6 (5)	34	0.80		0.2	
Central/2.1 (0.7)	MRD	19 (7)	42	0.53		0.05‡	
			38	0.39	31	0.002‡	0.01‡
	MpRD	16 (6)	37	0.55		0.06‡	
			41	0.51	27	0.006‡	0.01‡
Peripheral/2.2 (0.7)	MRD	13 (5)	31	0.55		0.04‡	
	MpRD	12 (6)	28	0.53		0.01‡	

Abbreviations: MRD = mean regional lung dose; MpRD = mean perfusion-weighted regional dose; other abbreviations as in Table 2. Data in parentheses are SD.

* Corresponding *p* values for parameter values for each lung region.

† *p* values for regions for which an offset parameter included for caudal tumors significantly improved the fit; for these regions, the fit parameters including this offset parameter are given.

‡ Statistically significant at $p \leq 0.05$.

the lung regions, the MpRD, averaged over all patients, was lower than, and for others it was equal, to, the MRD (Table 4). For individual cases, the MpRD could be greater than the MRD, but, on average, the MpRD was lower than the MRD in the irradiated areas, because perfusion of lung tissue adjacent to the tumor was often reduced.

Radiation pneumonitis

Good correlations between the MLD or MpLD and the incidence of RP were observed for the whole lung (Fig. 3A, B). The MRD in the posterior, caudal, ipsilateral, and both central and peripheral lung regions correlated significantly (*p* varied from 0.05 [central] to 0.002 [posterior] with the incidence of RP (Fig. 3 and Table 4). For the anterior, cranial, and contralateral lung, no correlation was observed between the MRD and the incidence of RP. To account for the influence of a greater RP incidence in patients with tumors in the lower lung region, an offset NTCP parameter was included in the NTCP model for patients with caudal tumors. The inclusion of an offset resulted in a significantly better fit of the model to the patient data for a number of lung regions. The parameter values and *p* values of the fitted NTCP curves and the offset NTCP parameter for caudal tumors (if significant) with corresponding *p* values are given in Table 4. In the analysis for the whole lung, the offset NTCP parameter was 28%, indicating that patients with caudal tumors had a 28% greater incidence of RP, irrespective of the MLD. The effect of this offset for the whole lung is illustrated in Fig. 4. The offset NTCP parameter is only valid in the studied dose range.

When the MpRD was used, similar results were again found for the whole lung (Fig. 3B) and for most subvolumes (Table 4). The MpRD of the posterior, ipsilateral, central, and peripheral regions showed good correlation with the probability of RP (*p* [including an offset NTCP parameter for caudal tumors, if significant] ranging from 0.05 [ipsilateral] to 0.006 [whole lung]). Again, no correlation was found for the contralateral lung (Table 4). For the caudal regions, the correlation was borderline statistically significant ($p = 0.07$). The most striking change using the perfusion-corrected MRD was, however, that the difference between the anterior and posterior part of the lung almost completely disappeared (Fig. 3C, D).

A wide variety in the values for TD_{50} was found (Table 4). Restricting the analysis to the regions in which a statistically significant correlation between the MRD or MpRD

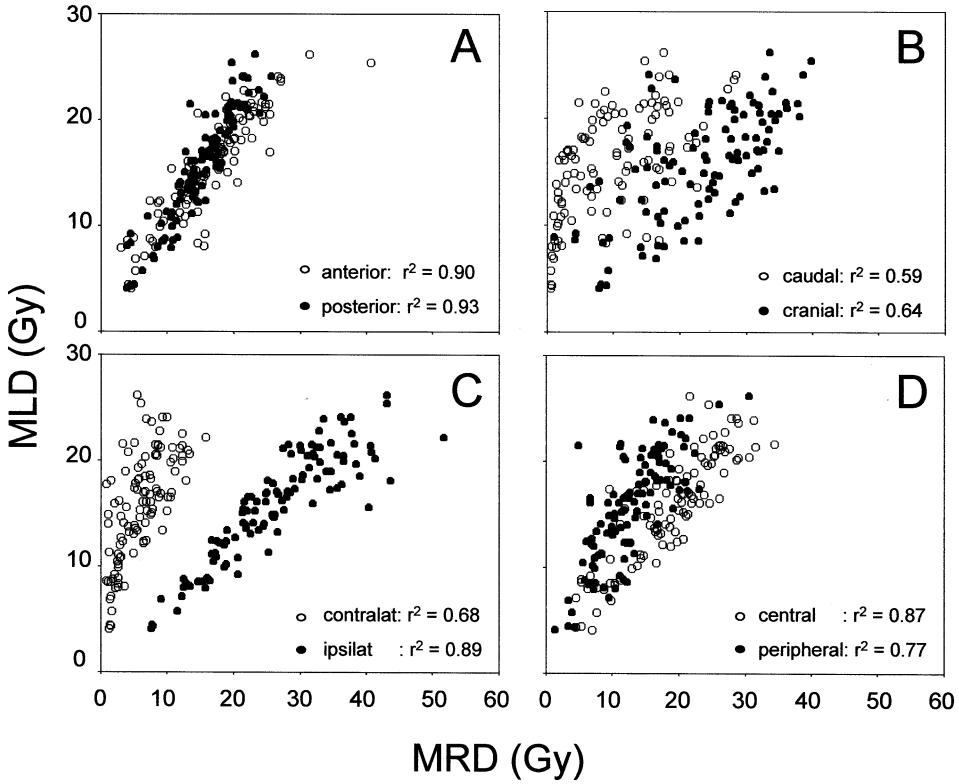

Fig. 2. Mean lung dose (MLD) vs. mean regional dose (MRD) for each patient and different lung regions; (A) anterior and posterior, (B) caudal and cranial, (C) contralateral and ipsilateral, and (D) central and peripheral.

and the incidence of RP was found, we observed that the TD_{50} tended to be somewhat greater in the central vs. peripheral regions. For anterior vs. posterior regions, the TD_{50} was similar after correction for regional perfusion differences. However, because the NTCP models using different MRDs or MpRDs were not nested, no statistical test was available to determine whether a particular MRD or MpRD was most significant for the prediction of RP.

DISCUSSION

Estimation of the NTCP for RP after treatment with high-dose RT is very important in dose-escalation studies for patients with NSCLC. The pathogenesis of RP is currently poorly understood, and it has been suggested that in addition to dosimetric parameters, patient-related factors (e.g., chemotherapy, pulmonary function, or coexisting lung disease) also influence the risk of RP.

The purpose of this study was to determine whether regional differences in radiation response were present in the lung, independent of the overall dose–volume parameters. The most striking finding was that patients with tumor in the caudal region had a statistically significantly greater risk of RP than patients with tumor in the cranial region. The observed difference in the dose–response relation between the anterior and posterior regions of the lung disappeared when we weighted the local dose with the local perfusion. A small difference was observed between the central and peripheral regions, but whether these differences were statistically significant could not be tested. Finally, the difference in the dose–response relation between the ipsilateral and contralateral lung was ascribed to the very low doses delivered to the contralateral lung and that the dose range delivered in the contralateral lung was too small.

Methods of analysis

To study the regional differences, we first analyzed whether a difference existed in the incidence of RP between patients with tumors in the opposite lung regions. To study the differences in more detail, we analyzed the MRD in relation to the incidence of RP, according to the study of Yorke *et al.* (10). They also calculated the MRDs for several regions in 63 patients treated for NSCLC. Logistic regression analysis was performed to determine whether a correlation could be found between the MRD and the incidence of RP Grade 3 (Radiation Therapy Oncology Group criteria, corresponding to Grade 2 Southwestern Oncology Group). The main limitation of using these MRDs was, however, that the probability of developing RP is not only dependent on the MRD, but also on the dose to the rest of the lungs. In our study, the MRDs all correlated significantly with the MLD (Fig. 2). Also, no large differences were found in the MLD between patients with tumors in opposite lung regions (Table 2), indicating that the observed differences in RP were probably not caused by interference with the dose to the rest of the lungs. However, because no statistical tests are available to

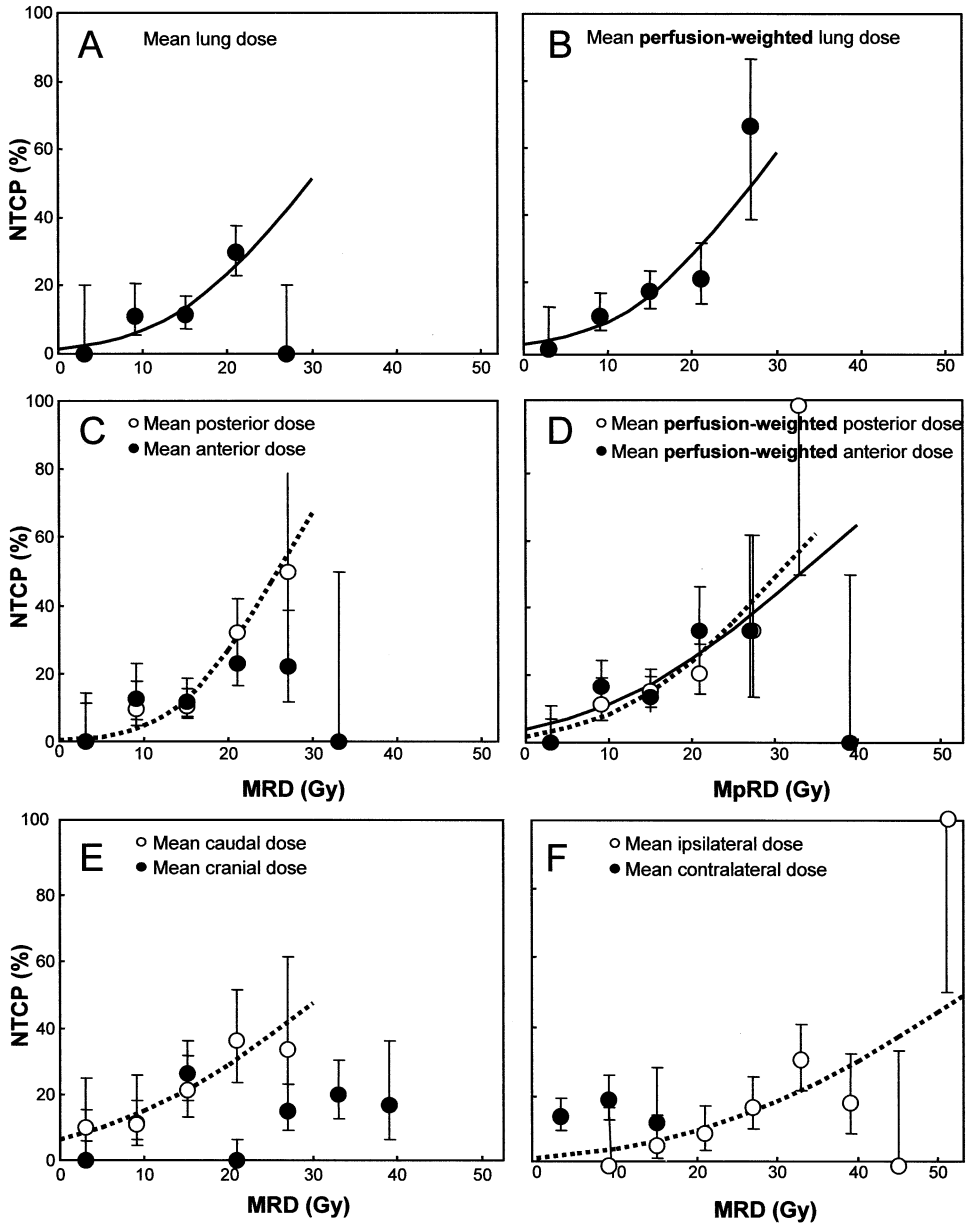

Fig. 3. Complication rate (NTCP) vs. mean dose to (A) total lung, (B) perfusion-weighted total lung, (C) posterior and anterior lung regions, (D) perfusion-weighted posterior and anterior lung regions, (E) caudal and cranial lung regions, and (F) ipsilateral and contralateral lungs. Curves fitted to data using maximal likelihood method. Coefficients with and without offset correction given in Table 4. Points obtained from data by calculating average fraction of RP incidence within 6-Gy bins. Error bars represent 68% confidence interval.

compare the fit to the NTCP models for the different regions, the results must be interpreted with caution.

Because it has been hypothesized that regional differences in sensitivity may be a result of a difference in functional subunit density (25) we used registered SPECT and CT data to estimate local functionality. This is the first study in which regional differences in the incidence of RP were studied using the "perfusion-corrected" regional dose.

Cranial–caudal differences

To account for the greater incidence of RP observed with caudal compared with cranial tumors (40% vs. 11%), a dose-independent offset NTCP parameter for caudal tumors was included in the NTCP model, resulting in a significantly improved fit for a number of lung regions (Table 4). Apart from the difference between patients with caudal and cranial tumors, we also analyzed the correlation between the MRD and the incidence of RP for the cranial and caudal regions. This showed a good correlation with the MRD in the caudal lung region, but no correlation at all in the cranial region. These data together suggest that the irradiation of caudal lung tissue carries a greater risk of developing RP than irradiation of the cranial lung. This observation is in line with the results of a study by Yorke *et al.* (10), which also

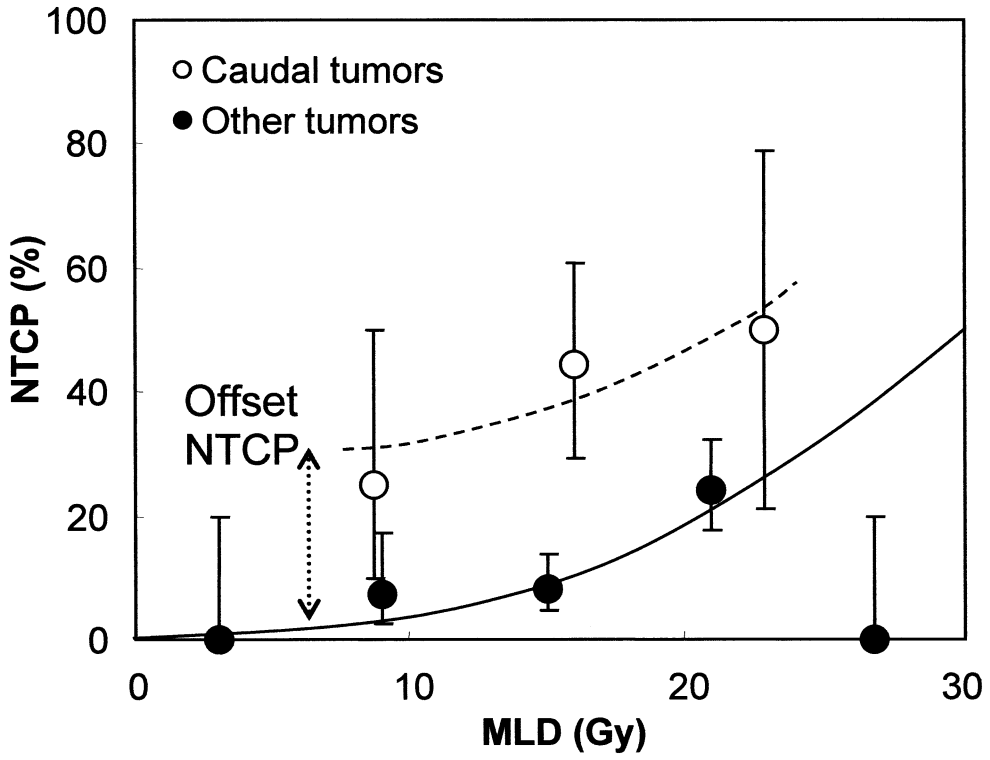

Fig. 4. MLD vs. NTCP for patients with caudal tumors (white circles) and tumors in other parts of lungs (black circles). Curves fitted to data using maximal likelihood method with offset parameter for caudal tumors. Coefficients given in Table 4. Error bars represent 68% confidence interval.

showed differences in dose–response relationship for the cranial and caudal lung subvolumes, with a strong correlation for the caudal MRD, and a lack of correlation for the cranial MRD. They also calculated other dose volume parameters, such as D_{eff} and f_{dam} (fraction of damaged functional subunits) for each region, all yielding a much better correlation in the caudal lung than in the cranial lung. In a study including 220 lung cancer patients, Yu *et al.* (26) could not confirm that the mean dose to the lower lung halves was more predictive of the development of RP than the mean dose to the superior half of the lungs. However, in Yu's study, patients with lower lobe tumors did not have a significant higher rate of RP as compared to patients with upper lobe tumors (24% vs. 18%, respectively).

Travis *et al.* (12) used a mouse model to study regional differences in lung radiosensitivity. The response of mouse lung to partial volume irradiation was heterogeneous and critically depended on the specific location of the irradiated subvolume in the lung (i.e., a given subvolume in the base was consistently more sensitive than the same subvolume in the apex using either breathing rate or lethality as an assay of RP). Khan *et al.* (13) found in a rat model that irradiation of the lower lung structure resulted in more DNA damage than irradiation of the upper lung. In addition, irradiation of the lower lung resulted in DNA damage in the shielded upper part of the lungs. However, irradiation of the upper lung did not result in DNA damage in the shielded lower lung, suggesting that, for example, circulating agents such as cytokines may play a role in the induction of radiation damage. It was suggested that partial irradiation of the heart and/or liver in the lower lobe tumors might mediate in this process (27). In all our patients with caudal lung tumors, the liver received a very low dose. In addition, we could not observe an obvious relation between the irradiated heart volume and the incidence of RP; however, the number of patients in this subgroup was very small.

Another mechanism that may explain the cranial–caudal difference is breathing-induced effects (10), especially in lower lung regions (28). Respiration-dependent motion alters the position of lung tumors and normal lung tissue so that more lung tissue is actually irradiated to a low dose than estimated from the "static" dose distribution. Modeling of motion effects and its influence on the dose distribution is a topic of ongoing research.

Anterior and posterior differences

Although a difference in the incidence of RP was observed for patients with anterior and posterior tumors, this difference did not reach statistical significance (Table 2). Nevertheless, we did find a different response of these regions in the sense that a very good correlation was found between the MRD and the incidence of RP for the posterior regions and no correlation at all for the anterior regions.

An explanation may be that this difference was due to a difference in regional function. Because gravity reallocates perfusion to the posterior (29, 30) and because patients were scanned and treated in the supine position, the posterior

region was much better perfused. Incorporating the local perfusion data in the MRD, the difference between the anterior and posterior regions completely disappeared (Fig. 3c, d). This suggests that the posterior region may not be more sensitive, *per se*, but that it may only be more sensitive because of better perfusion. In that case, it should only be more sensitive when the patient is in the supine position. It could be postulated that in the presence of a better perfusion, more oxygen is present, and more oxygen radicals can be formed.

Central–peripheral differences

Although no difference in the incidence of RP was found between patients with central and peripheral tumors, the MLD was significantly different for these patient groups (17 Gy vs. 12 Gy; Table 2). In addition, the TD_{50} for the central MRD was greater than for the peripheral MRD (38 Gy and 31 Gy, respectively), also suggesting that peripheral tissue may be more radiosensitive. However, from these data, it could not be tested whether this really means a statistically significant difference in the dose–response relation. In addition, if present, the difference seemed to be modest compared with the difference between the caudal and cranial regions.

Contralateral–ipsilateral differences

We found a different dose–response relation for the contralateral and ipsilateral lung that could not be explained by either a difference in the MLD between these groups or by a difference in local perfusion. However, the MRDs did show a large difference, with the average MRD of the contralateral lung much lower than the average MRD of the ipsilateral lung (6 Gy vs. 26 Gy). These data are very similar to the results of Yorke *et al* (10), who also found a difference in the dose–response effect and a large difference in the MRD (6.6 Gy vs. 26.3 Gy). The MRD of 6 Gy probably contributed too little to the MLD to be able to detect a dose–response effect.

All dose calculations in this study were performed using an equivalent path length algorithm. As previously published (31), this algorithm does not account for the increased range of secondary electrons in low-density lung tissue. In the contralateral lung, we found a consistent average overestimate of the dose of about 30%.

Another finding was that the TD_{50} of the ipsilateral lung was much greater than the TD_{50} of both lungs together (57 Gy vs. 30 Gy. respectively). The TD_{50} of both lungs was comparable to the TD_{50} values previously published by our group (14, 31). This finding indicates that different values for TD_{50} should apply if one considers both lungs as one organ or both lungs separately.

CONCLUSION

We found that irradiation of caudal tumors is associated with a greater incidence of RP than irradiation of other tumor locations, irrespective of dose–volume parameters. This difference could not be explained by a difference in regional perfusion. It is not yet clear whether these data mean a real difference in radiosensitivity exists or that the MRD in the caudal region is underestimated owing to breathing movements. Respiration-correlated CT studies are currently underway to study this issue in more detail. In addition, we found a difference in the dose–response effect between the anterior and posterior lung regions, which was probably due to the better perfusion of the posterior lung because the patient was in the supine position.

REFERENCES

1. Gagliardi G, Bjohle J, Lax I, *et al.* Radiation pneumonitis after breast cancer irradiation: Analysis of the complication probability using the relative seriality model. *Int J Radiat Oncol Biol Phys* 2000;46:373–381.
2. Graham MV, Drzymala RE, Jain NL, *et al.* Confirmation of dose–volume histograms and normal tissue complication probability calculations to predict pulmonary complications after radiotherapy for lung cancer. *Int J Radiat Oncol Biol Phys* 1994;30:198.
3. Hernando ML, Marks LB, Bentel GC, *et al.* Radiation-induced pulmonary toxicity: A dose–volume histogram analysis in 201 patients with lung cancer. *Int J Radiat Oncol Biol Phys* 2001; 51:650–659.
4. Jackson A, Kutcher GJ, Yorke ED. Probability of radiation-induced complications for normal tissues with parallel architecture subject to non-uniform irradiation. *Med Phys* 1993;20: 613–625.
5. Kwa SL, Lebesque JV, Theuws JC, *et al.* Radiation pneumonitis as a function of mean lung dose: An analysis of pooled data of 540 patients. *Int J Radiat Oncol Biol Phys* 1998;42: 1–9.
6. Martel MK, Ten Haken RK, Hazuka MB, *et al.* Dose–volume histogram and 3-D treatment planning evaluation of patients with pneumonitis. *Int J Radiat Oncol Biol Phys* 1994;28:575–581.
7. Yorke ED, Kutcher GJ, Jackson A, *et al.* Probability of radiation-induced complications in normal tissues with parallel architecture under conditions of uniform whole or partial organ irradiation. *Radiother Oncol* 1993;26:226–237.
8. Graham MV, Purdy JA, Emami B, *et al.* Clinical dose–volume histogram analysis for pneumonitis after 3D treatment for non–small-cell lung cancer (NSCLC). *Int J Radiat Oncol Biol Phys* 1999;45:323–329.
9. Graham MV, Purdy JA, Emami B, *et al.* Preliminary results of a prospective trial using three dimensional radiotherapy for lung cancer. *Int J Radiat Oncol Biol Phys* 1995;33:993–1000.
10. Yorke ED, Jackson A, Rosenzweig KE, *et al.* Dose-volume factors contributing to the incidence of radiation pneumonitis in non–small-cell lung cancer patients treated with three-dimensional conformal radiation therapy. *Int J Radiat Oncol Biol Phys* 2002;54:329–339.
11. Moiseenko VV, Battista JJ, Hill RP, *et al.* In field and out-of-field effects in partial volume lung irradiation in rodents: Possible correlation between early DNA damage and functional endpoints. *Int J Radiat Oncol Biol Phys* 2000;48:1539–1548.
12. Travis EL, Liao ZX, Tucker SL. Spatial heterogeneity of the

volume effect for radiation pneumonitis in mouse lung. *Int J Radiat Oncol Biol Phys* 1997;38:1045–1054.
13. Khan MA, Van Dy, J, Yeun, *et al.* Partial volume rat lung irradiation: Assessment of early DNA damage in different lung regions and effect of radical scavengers. *Radiother Oncol* 2003;66:95–102.
14. Seppenwoolde Y, Lebesque JV, De Jaeger K, *et al.* Comparing different NTCP models that predict the incidence of radiation pneumonitis: Normal tissue complication probability. *Int J Radiat Oncol Biol Phys* 2003;55:724–735.
15. Belderbos JS, De Jaeger K, Heemsbergen WD, *et al.* First results of a phase I/II dose escalation trial in non-small cell lung cancer using three-dimensional conformal radiotherapy. *Radiother Oncol* 2003;66:119–126.
16. Seppenwoolde Y, Muller SH, Theuws JC, *et al.* Radiation dose-effect relations and local recovery in perfusion for patients with non–small-cell lung cancer. *Int J Radiat Oncol Biol Phys* 2000;47:681–690.
17. Kwa SL, Theuws JC, van Herk M, *et al.* Automatic three-dimensional matching of CT-SPECT and CT-CT to localize lung damage after radiotherapy. *J Nucl Med* 1998;39:1074–1080.
18. Chang LT. A method for attenuation correction in radionuclide computed tomography. *EEE Trans Nucl Sci* 1978;25: 638–643.
19. Damen EM, Muller SH, Boersma LJ, *et al.* Quantifying local lung perfusion and ventilation using correlated SPECT and CT data. *J Nucl Med* 1994;35:784–792.
20. Boersma LJ, Damen EM, de Boer RW, *et al.* Dose-effect relations for local functional and structural changes of the lung after irradiation for malignant lymphoma. *Radiother Oncol* 1994;32:201–209.
21. Lebesque JV, Keus RB. The simultaneous boost technique: The concept of relative normalized total dose. *Radiother Oncol* 1991;22:45–55.
22. Newcomb CH, van Dyk J, Hill RP. Evaluation of isoeffect formulae for predicting radiation-induced lung damage. *Radiother Oncol* 1993;26:51–63.
23. Maciejewski B, Taylor JM, Withers HR. Alpha/beta value and the importance of size of dose per fraction for late complications in the supraglottic larynx. *Radiother Oncol* 1986;7:323–326.
24. Clayton D, Hills M. Statistical models in epidemiology. New York: Oxford University Press; 1993.
25. Tucker SL, Liao ZX, Travis EL. Estimation of the spatial distribution of target cells for radiation pneumonitis in mouse lung. *Int J Radiat Oncol Biol Phys* 1997;38:1055–1066.
26. Yu X, Zhou S, Kahn D, *et al.* Predicting RT-induced pulmonary symptoms based on the dose to the superior vs. inferior lung in patients irradiated for lung cancer [Abstract]. *Int J Radiat Oncol Biol Phys* 2003;57(Suppl.):S415.
27. Marks LB. Dosimetric predictors of radiation-induced lung injury. *Int J Radiat Oncol Biol Phys* 2002;54:313–316.
28. Seppenwoolde Y, Shirato H, Kitamura K, *et al.* Precise and real-time measurement of 3D tumor motion in lung due to breathing and heartbeat, measured during radiotherapy. *Int J Radiat Oncol Biol Phys* 2002;53:822–834.
29. Theuws JC, Kwa SL, Wagenaar AC, *et al.* Dose-effect relations for early local pulmonary injury after irradiation for malignant lymphoma and breast cancer. *Radiother Oncol* 1998;48:33–43.
30. Zwikler MP, Peters TM, Michel RP. Effects of pulmonary fibrosis on the distribution of edema: Computed tomographic scanning and morphology. *Am J Respir Crit Care Med* 1994; 149:1266–1275.
31. De Jaeger K, Hoogeman M, Engelsman M, *et al.* Incorporating an improved dose computation algorithm in conformal radiotherapy of lung cancer: Re-evaluation of dose in lung tissue. *Radiother Oncol* 2003;69:1–10.